Terahertz instability of surface optical-phonon polaritons that interact with surface plasmon polaritons in the presence of electron drift

O. Sydoruk,[1] E. Shamonina,[2] V. Kalinin,[3] and L. Solymar[1]
[1]*Department of Electrical and Electronic Engineering, Optical and Semiconductor Devices Group, Imperial College, Exhibition Road, London SW7 2BT, United Kingdom*
[2]*Erlangen Graduate School in Advanced Optical Technologies, University of Erlangen-Nuremberg, Paul-Gordan Str. 6, D-91052 Erlangen, Germany*
[3]*Transense Technologies Ltd., Upper Heyford, Bicester, Oxon OX25 5HD, United Kingdom*

(Received 17 May 2010; accepted 16 August 2010; published online 15 October 2010)

Traveling-wave interaction between optical phonons and electrons drifting in diatomic semiconductors has potential for amplification and generation of terahertz radiation. Existing models of this interaction were developed for infinite materials. As a more practically relevant configuration, we studied theoretically a finite semiconductor slab surrounded by a dielectric. This paper analyzes the optical-phonon instability in the slab including the Lorentz force and compares it to the instability in an infinite material. As the analysis shows, the slab instability occurs because of the interaction of surface optical-phonon polaritons with surface plasmon polaritons in the presence of electron drift. The properties of the instability depend on the slab thickness when the thickness is comparable to the wavelength. For large slab thicknesses, however, the dispersion relation of the slab is similar to that of an infinite material, although the coupling is weaker. The results could be used for the design of practical terahertz traveling-wave oscillators and amplifiers. © *2010 American Institute of Physics*. [doi:10.1063/1.3486524]

I. INTRODUCTION

Developing sources of terahertz radiation is one of the major tasks of today's terahertz science and technology. Recent years have seen considerable progress in this direction, and many ways to generate terahertz are now known. One of the most popular and well-developed methods is the use of photoconductive switches, where radiation is generated by illuminating a photoconductive material with low carrier life time by a femtosecond laser.[1] Another method, receiving considerable attention, is generation by quantum-cascade lasers.[2,3] Vacuum electronic sources are being developed for high-power applications.[4] On the other hand, semiconductor plasmas[5] are attractive for lower output powers. For example, a semiconductor oscillator was studied theoretically[6] and experimentally[7,8] where terahertz radiation is generated by reflection of plasma waves from the device boundaries.

Moreover, because plasma frequencies in semiconductors can lie in the terahertz range, semiconductor plasmas have potential for terahertz solid-state analogs of vacuum traveling-wave tubes and backward-wave oscillators. In these devices, electrons drifting in a semiconductor interact with slow backward or forward electromagnetic waves.[9–11] In vacuum tubes, the electromagnetic waves are usually slowed down by a helix or another artificial slow-wave structure.[12] In solids, a possible choice for the slow wave is optical phonons, which are particularly suited for terahertz applications because optical-phonon frequencies of most diatomic semiconductors lie in the terahertz range. High-mobility diatomic semiconductors, such as InSb, can support both optical phonons and drifting electrons. Traveling-wave interaction between the phonons and electrons drifting in the same material could lead to instability and thus it can be used to amplify and generate terahertz radiation. First considered theoretically in the 1960s,[13–16] this effect has been recently revisited by Riyopoulos, who derived and analyzed the dispersion relation in an infinite material using the hydrodynamic[17] and the kinetic[18] approaches.

While previous studies of this optical-phonon instability considered infinite materials, practical realizations are, of course, finite and may have properties different from those of infinite ones. First, the gain in a finite configuration could depend on its dimensions. Second, boundaries between a semiconductor and a dielectric in a finite configuration can support surface optical-phonon polaritons (SOPPs) and surface plasmon polaritons (SPPs),[19,20] whose properties differ from those of their bulk counterparts. In the third place, finite configurations can support electron movement not only in the longitudinal direction, parallel to the applied electric field, but also in the transverse directions. Due to this movement, magnetic field, which does not play a role in infinite materials, may influence the properties of finite configurations.

The obvious choice of a finite system is a semiconductor slab confined in one direction but infinite in the other two, see Fig. 1. This paper discusses the instability in the slab arising when SOPPs interact with drifting electrons.

Instability means that signals in a system grow in time. For a harmonic time-varying signal of the form $\exp(j\omega t)$ (where ω is the frequency, t is the time, and j is the imaginary unit), it implies complex frequency with a negative value of the imaginary part. Whether such solutions exist can be determined by solving the dispersion equation, relating wave numbers and frequencies of the waves propagating in the system. To study the slab instability, we derive the dispersion equation in Sec. II and then analyze it in Sec. III,

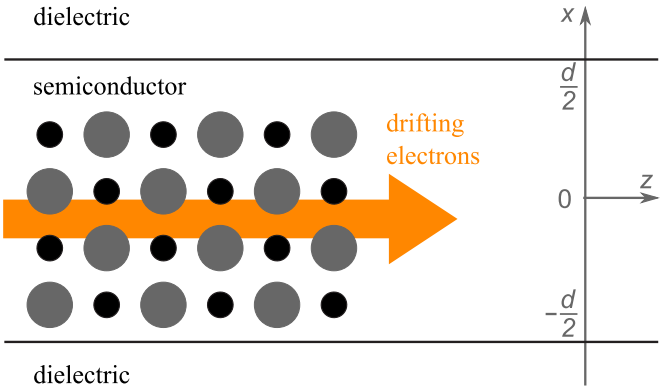

FIG. 1. (Color online) A semiconductor slab of thickness d is surrounded by a dielectric. The semiconductor supports optical phonons and drifting electrons. Interaction between them can lead to a terahertz instability.

where we determine conditions for the optical-phonon instability, discuss how the gain depends on the slab thickness and the plasma frequency, and find the field distributions in the slab. In Sec. IV, we draw conclusions.

II. DERIVATION OF THE DISPERSION RELATION

To derive the dispersion relation, we solve Maxwell's equations in the semiconductor and the dielectric subject to boundary conditions. In the presence of ac electric, **E**, and ac magnetic, **H**, fields, the equation of motion can be written as

$$\frac{\partial \mathbf{v}}{\partial t} + (\mathbf{v}\cdot\nabla)\mathbf{v} = \frac{e}{m^*}(\mathbf{E} + \delta_{\mathrm{L}}\mu_0 \mathbf{v}\times\mathbf{H}), \tag{1}$$

where $\mathbf{v}$ is the electron velocity, e is the electron charge, m^* is the electron effective mass, and μ_0 is the free space permeability. The term with the magnetic field $\mathbf{H}$ in Eq. (1) describes the Lorentz force. Later, we will compare the dispersion relations derived with and without the Lorentz force. For this reason, we multiplied the Lorentz force in Eq. (1) by δ_{L} that is equal to 0 when the Lorentz force is neglected and to 1 when it is taken into account. We also ignored electron collisions and diffusion in the equation of motion, which could be justified for high-mobility semiconductors at low temperatures. For a discussion of the effects of diffusion, see also Ref. 18.

Moving electrons create a current with the density

$$\mathbf{J} = en\mathbf{v}, \tag{2}$$

where n is the electron density. Equations (1) and (2) are nonlinear. To linearize them and obtain the dispersion relation, we assume, as it is usually done, that the electron density and velocity have a constant part and a small time-varying part,

$$\begin{aligned} n &= n_0 + \tilde{n}\exp(\mathrm{j}\omega t), \quad |\tilde{n}| \ll n_0, \\ v_z &= v_0 + \tilde{v}_z \exp(\mathrm{j}\omega t), \quad |\tilde{v}_z| \ll v_0, \\ v_x &= \tilde{v}_x \exp(\mathrm{j}\omega t), \quad |\tilde{v}_x| \ll v_0, \end{aligned} \tag{3}$$

where v_0 is the electron drift velocity, see Fig. 1, and n_0 is the dc electron density, which we take constant across the slab. Then, substituting Eq. (3) into Eqs. (1) and (2), we ignore products of small quantities, so that the z-component of the ac current density, for example, has the form $J_z = en_0\tilde{v}_z + e\tilde{n}v_0$.

Effects of the optical phonons can be included into the permittivity of the semiconductor. We take the optical-phonon permittivity in its usual form,

$$\varepsilon_{\mathrm{phon}} = \varepsilon_\infty \frac{\omega^2 - \omega_{\mathrm{L}}^2}{\omega^2 - \omega_{\mathrm{T}}^2}, \tag{4}$$

where ω_{L} and ω_{T} are the longitudinal and transverse optical-phonon frequencies, and ε_∞ is the high-frequency permittivity. Assuming TM waves with the field components E_z, E_x, and H_y, substituting Eqs. (1)–(4) into Maxwell's equations, and assuming the spatial variation of all ac quantities in the form $\exp[-\mathrm{j}(k_z z + k_{xs}x)]$, we obtain the following dispersion relation:

$$k_z^2 + k_{xs}^2 = k_0^2 \varepsilon_{\mathrm{eff1}}, \tag{5}$$

where $k_0 = \omega/c_0$ (c_0 is the light velocity) and

$$\varepsilon_{\mathrm{eff1}} = \varepsilon_{\mathrm{phon}} - \varepsilon_\infty \frac{\omega_{\mathrm{p}}^2}{[\omega - k_z v_0][\omega - (1-\delta_{\mathrm{L}})k_z v_0]}. \tag{6}$$

Here, ω_{p} is the plasma frequency defined as

$$\omega_{\mathrm{p}}^2 = \frac{e^2 n_0}{\varepsilon_0 \varepsilon_\infty m^*}, \tag{7}$$

where ε_0 is the free-space permittivity.

In the dielectric, we assume the spatial variation of the fields in the form $\exp[-\mathrm{j}(k_z z + k_{xd}x)]$. The solution of Maxwell's equations gives then the standard dispersion relation,

$$k_z^2 + k_{xd}^2 = k_0^2 \varepsilon_{\mathrm{d}}, \tag{8}$$

where ε_{d} is the permittivity of the dielectric. Comparing Eqs. (5) and (8), we can call $\varepsilon_{\mathrm{eff1}}$ in Eq. (5) an effective permittivity of the semiconductor. This effective permittivity depends on whether the Lorentz force is taken into account, see Eq. (6).

For the fields in the dielectric to vanish at infinity, k_{xd} must be imaginary, such that $k_{xd} = -\mathrm{j}\kappa_{xd}$. Similarly, we will assume imaginary k_{xs} in the semiconductor, $k_{xs} = -\mathrm{j}\kappa_{xs}$. Then, Eqs. (5) and (8) change to

$$\begin{aligned} k_z^2 - \kappa_{xs}^2 &= k_0^2 \varepsilon_{\mathrm{eff1}}, \\ k_z^2 - \kappa_{xd}^2 &= k_0^2 \varepsilon_{\mathrm{d}}. \end{aligned} \tag{9}$$

To obtain the complete dispersion relation for the slab, we have to take boundary conditions into account. These conditions should include the ac charges accumulating on the boundaries due to the transverse movement of the electrons. The surface charge density, ρ_{surf}, can be expressed as[12]

$$\rho_{\mathrm{surf}} = \frac{J_x}{\mathrm{j}(\omega - k_z v_0)}, \tag{10}$$

and the corresponding surface current density as $J_{\mathrm{surf}} = v_0 \rho_{\mathrm{surf}}$. It needs to be emphasized here that in the case of slab with drifting electrons, both surface charge and surface

current should be taken into account. In our model, the boundary condition for the magnetic field takes then the form

$$H_{yd}|_{x=\pm d/2} = \frac{\varepsilon_{\text{eff2}}}{\varepsilon_{\text{eff1}}} H_{ys}|_{x=\pm d/2}, \tag{11}$$

where H_{yd} and H_{ys} are the magnetic fields in the dielectric and in the semiconductor, and

$$\varepsilon_{\text{eff2}} = \varepsilon_{\text{phon}} - \varepsilon_{\infty} \frac{\omega_p^2}{(\omega - k_z v_0)^2}. \tag{12}$$

When deriving Eq. (12) in the presence of the Lorentz force, $\delta_L = 1$ in Eq. (1), we assumed that v_0^2/c^2, the relativistic correction, is much smaller than unity.

Using Eq. (11) together with the condition that E_z is continuous at the boundaries, we can write the slab dispersion relation as

$$\tanh\frac{\kappa_{xd} d}{2} = -\frac{\kappa_{xs}\varepsilon_d}{\kappa_{xd}\varepsilon_{\text{eff2}}}, \qquad \coth\frac{\kappa_{xd} d}{2} = -\frac{\kappa_{xs}\varepsilon_d}{\kappa_{xd}\varepsilon_{\text{eff2}}}, \tag{13}$$

respectively. The form of Eq. (13) is identical to that of the dispersion relations of SPPs and SOPPs.[19,20] In the following, we will refer to the first solution as tanh-mode and to the second one as coth-mode.

Equation (13) can be simplified. First, we notice that the electron drift velocities achievable in semiconductors are much smaller than the light velocity c_0 (for example, the highest drift velocity reported for InSb is[21] $v_{0\,\max} \approx c_0/300$). Estimating the wave number at which the instability occurs as $k_z = \text{Re}\,\omega/v_0$, we have $k_z \gg k_0$, and given $\text{Im}\,\omega \neq 0$, the term proportional to k_0 in Eq. (9) can be ignored, yielding

$$\kappa_{xs} = \kappa_{xd} = k_z. \tag{14}$$

Equation (14) transforms Eq. (13) into

$$\tanh\frac{k_z d}{2} = -\frac{\varepsilon_d}{\varepsilon_{\text{eff2}}}, \qquad \coth\frac{k_z d}{2} = -\frac{\varepsilon_d}{\varepsilon_{\text{eff2}}}, \tag{15}$$

respectively. Equations (14) and (15) have the same form regardless of whether we take the Lorentz force in the equation of motion, Eq. (1). It means that, provided Eq. (14) is true, including the Lorentz force does not influence the instability.

A further simplification comes from considering large slab thicknesses, d. If $k_z d \gg 1$, $\tanh(k_z d/2) \approx \coth(k_z d/2) \approx 1$, and Eq. (15) yields $\varepsilon_d = -\varepsilon_{\text{eff2}}$. Taking into account the definition of $\varepsilon_{\text{eff2}}$, Eq. (12),

$$1 - \frac{\omega_L^2 - \omega_T^2}{\omega^2 - \omega_T^2} - \frac{\omega_p^2}{(\omega - k_z v_0)^2} = -\frac{\varepsilon_d}{\varepsilon_\infty}, \tag{16}$$

followed by

$$(\omega_L^2 - \omega_T^2)(\omega - k_z v_0)^2 + \omega_p^2(\omega^2 - \omega_T^2) = \left(1 + \frac{\varepsilon_d}{\varepsilon_\infty}\right)(\omega^2 - \omega_T^2)(\omega - k_z v_0)^2. \tag{17}$$

Rearranging the terms, we obtain

$$(\omega - k_z v_0)^2 \left[(\omega_L^2 - \omega_T^2) - \left(1 + \frac{\varepsilon_d}{\varepsilon_\infty}\right)(\omega^2 - \omega_T^2)\right] + \omega_p^2(\omega^2 - \omega_T^2) = 0. \tag{18}$$

Then, we multiply both terms by $1 + \varepsilon_d/\varepsilon_\infty$ and expand the second term by writing

$$\left(1 + \frac{\varepsilon_d}{\varepsilon_\infty}\right)(\omega^2 - \omega_T^2) = \left(1 + \frac{\varepsilon_d}{\varepsilon_\infty}\right)(\omega - \omega_T^2) - (\omega_L^2 - \omega_T^2) + (\omega_L^2 - \omega_T^2)$$

to obtain

$$\left[(\omega_L^2 - \omega_T^2) - \left(1 + \frac{\varepsilon_d}{\varepsilon_\infty}\right)(\omega^2 - \omega_T^2)\right]\left[(\omega - k_z v_0)^2\left(1 + \frac{\varepsilon_d}{\varepsilon_\infty}\right) - \omega_p^2\right] = -\omega_p^2(\omega_L^2 - \omega_T^2). \tag{19}$$

Diving both sides of this expression by $(1 + \varepsilon_d/\varepsilon_\infty)^2$, we recast the dispersion relation in the form

$$\left[\omega^2 - \frac{\varepsilon_\infty \omega_L^2 + \varepsilon_d \omega_T^2}{\varepsilon_\infty + \varepsilon_d}\right]\left[(\omega - k_z v_0)^2 - \frac{\varepsilon_\infty \omega_p^2}{\varepsilon_\infty + \varepsilon_d}\right] = \frac{\varepsilon_\infty^2}{(\varepsilon_\infty + \varepsilon_d)^2}\omega_p^2(\omega_L^2 - \omega_T^2), \tag{20}$$

which is standard for coupled-wave interactions. The first bracket on the left-hand side corresponds to the SOPPs. The second bracket corresponds to the SPPs in the presence of drift. It has the form analogous to the dispersion relation of bulk space-charge waves with the reduced plasma frequency,[12,22]

$$\omega_p^{(\text{reduced})} = \sqrt{\frac{\varepsilon_\infty}{\varepsilon_\infty + \varepsilon_d}}\,\omega_p. \tag{21}$$

The term on the right-hand side is the coupling coefficient. The dispersion relation Eq. (20) does not depend on the slab thickness. It means that the surface waves propagating on the different sides of the slab do not interact with each other; the slab behaves like a semi-infinite material.

III. ANALYSIS OF THE DISPERSION RELATION

Dispersion relation Eq. (13) and its simplified forms Eqs. (15) and (20) describe the interaction between SOPPs and drifting SPPs. Analyzing the dispersion relation, we can determine when this interaction becomes unstable.[23] To do so, we solve the dispersion relation for the frequency ω, assuming real wave numbers, k_z. The resulting values of ω are, in general, complex. An instability is signaled by solutions with $\text{Im}\,\omega < 0$, and the value $|\text{Im}\,\omega|$ shows how fast the corresponding wave grows in time, i.e., characterizes the temporal gain.

TABLE I. Parameters used in numerical calculations correspond to InSb.

Longitudinal phonon frequency, $f_L=\omega_L/(2\pi)$	5.71 THz
Transverse phonon frequency, $f_L=\omega_L/(2\pi)$	5.37 THz
High frequency dielectric constant, ε_∞	15.7
Electron effective mass, m^*	$0.014m_0$
Drift velocity, v_0	$c_0/300=10^6$ m/s
Lattice constant, a	0.648 nm

In this section, we analyze the dispersion relation, first for large, and then for small slab thicknesses. For numerical calculations, we take parameters corresponding to InSb, see Table I.

A. Instability at large slab thicknesses

As argued above, the dispersion relation Eq. (13) can be simplified for large slab thicknesses to the form of Eq. (20). The corresponding condition is $k_z d \gg 1$. Assuming $k_z = \omega_L/v_0$ and taking the parameters from Table I, we obtain the estimate $d \gg 30$ nm.

We start analyzing the dispersion relation by setting the electron drift velocity to zero. Then, the interaction between the SPPs and SOPPs can only be passive. The dispersion curves given by Eq. (20) are two horizontal lines, as seen in Fig. 2, for $f_p=\omega_p/(2\pi)=1$ THz and $\varepsilon_d=1$. They correspond to the frequencies 5.70 and 0.91 THz, which differ from f_L (5.71 THz) and f_p (1 THz) due to the plasmon-phonon interaction and the presence of the boundary. The wave number in Fig. 2 is normalized to the lattice constant, a.

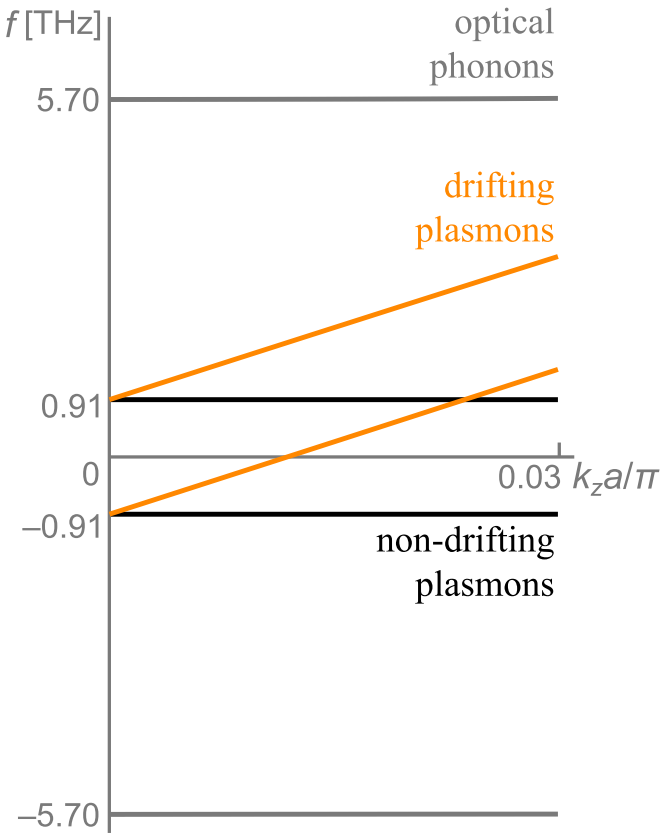

FIG. 2. (Color online) In the presence of drift, the dispersion curves for the SPPs rotate by an amount proportional to the drift velocity. There is no instability when the drift velocity is zero or small.

Figure 2 was plotted using Eq. (20), but as confirmed by numerical calculations, the complete dispersion equation, Eq. (13), gives the same result for the range of the wave numbers shown. However, for small wave numbers comparable with k_0 (not seen in the scale of Fig. 2) solutions of Eq. (13) deviate from straight lines and follow the usual SOPP and SPP dispersion curves, the latter rising from $\omega=0$, $k=0$.[19,20] These solutions are of no interest in the present context, and we will not show them.

When the electrons drift, the SPP dispersion curves rotate counterclockwise by an amount proportional to the value of the drift velocity, as shown in Fig. 2 by orange lines for $v_0=c_0/3000$. This value of the drift velocity is too low for the SPP dispersion curves to cross the phonon dispersion curves. Consequently, there is still no instability in the region shown.

As the drift velocity increases, the dispersion curves of the SPPs can cross those of the SOPPs giving rise to the optical-phonon instability, as shown in Figs. 3(a) and 3(b) for $v_0=c_0/300$. The other parameters are the same as in Fig. 2. The presence of the instability is confirmed by the negative values of Im ω, shown in Fig. 3(b). The instability exists between 5.20 and 6.02 THz; the temporal gain is maximal at 5.62 THz.

As follows from Eq. (20), the coupling between SOPPs and SPPs increases with increase of the plasma frequency. Larger coupling coefficients lead to stronger instabilities, with larger gains and wider frequency ranges. This effect is demonstrated in Figs. 3(c) and 3(d) for $f_p=5.5$ THz, which lies between f_L and f_T, and Figs. 3(e) and 3(f) for $f_p=10$ THz, which is larger than f_L. The maximum value of $-\mathrm{Im}\, f$ increases from 0.4 THz for $f_p=1$ THz to 0.9 THz for $f_p=5.5$ THz and further to 1.2 THz for $f_p=10$ THz. The value of the frequency at which this maximum is reached is roughly independent of the plasma frequency, but the unstable frequency range increases from 0.82 to 1.83 THz and to 2.44 THz.

On the other hand, increasing the permittivity of the dielectric, ε_d, decreases the coupling coefficient and also changes the coupled phonon-plasmon frequencies, see Eq. (20). Smaller coupling coefficients lead to weaker instabilities, as shown in Fig. 4 for $\varepsilon_d=11.6$ (corresponding to silicon[24]) and $f_p=1$ THz. The instability occurs between 5.23 and 5.8 THz, and the maximum value of $-\mathrm{Im}\, f$ is 0.27 THz, smaller than the values corresponding to $\varepsilon_d=1$, see Figs. 3(a) and 3(b).

The polynomial form of the dispersion relation Eq. (20) allows direct comparison between the dispersion relation for the slab and the dispersion relation for an infinite material. The dispersion relation for an infinite material has the form[17,18]

$$[\omega^2-\omega_L^2][(\omega-k_z v_0)^2-\omega_p^2]=\omega_p^2(\omega_L^2-\omega_T^2). \quad (22)$$

Apart from different frequencies for the bulk and the surface waves, Eqs. (20) and (22) differ in the coupling coefficient. The coupling coefficient for the slab is smaller than that of

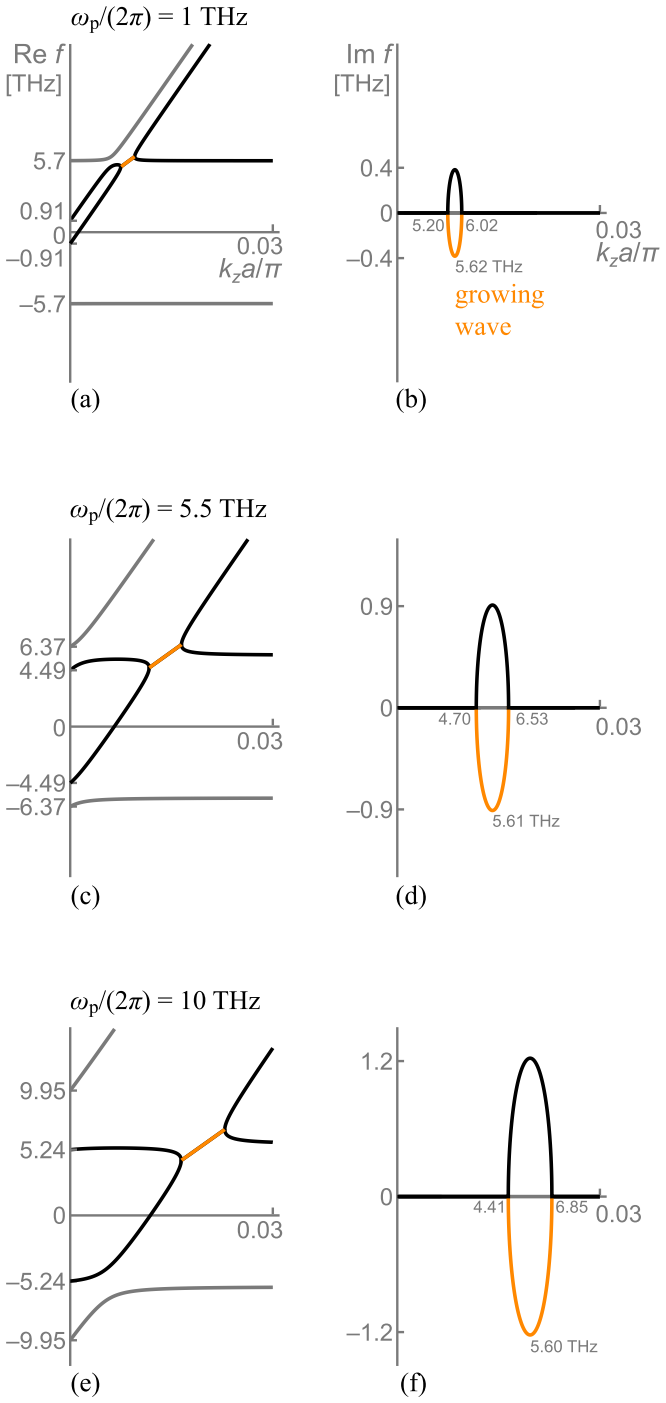

FIG. 3. (Color online) The interaction between SOPPs and SPPs leads to a terahertz instability when the drift velocity is sufficiently large. The instability is signaled by the negative values of Im f. The instability is stronger for higher values of the plasma frequency. [(a), (c), and (e)] Real and [(b), (d), and (f)] imaginary parts of the frequency against the wave number normalized to the lattice constant, a.

the infinite material which leads, as could be expected, to weaker instability. However, if $\varepsilon_\infty \gg \varepsilon_d$, the difference between the coupling coefficients is small, and the two instabilities behave identically.

B. Instability at small slab thicknesses

When the slab thickness decreases and becomes comparable to the value $d=v_0/\omega_L$ (30 nm for our parameters), the approximation of Eq. (20) fails. One has to take the complete

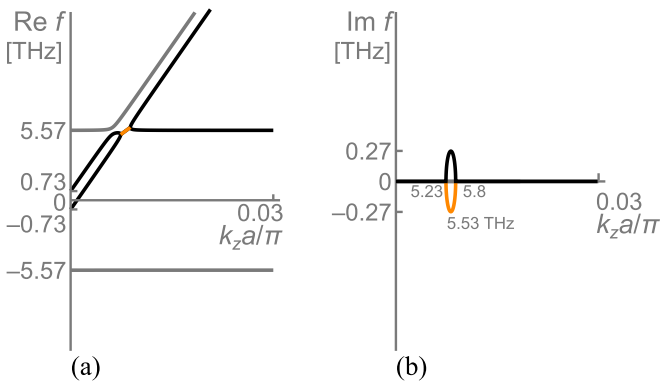

FIG. 4. (Color online) Increasing the permittivity of the dielectric surrounding the slab leads to weaker instability, with narrower frequency range and smaller growth rates, as shown on the dispersion diagrams for $\varepsilon_d=11.6$, compare with Figs. 3(a) and 3(b).

dispersion relations in the form of Eq. (13). As numerical calculations for small thicknesses show, dispersion diagrams for both tanh-mode and coth-mode, Eq. (13), look qualitatively similar to those of Fig. 3; the largest difference occurs at small wave numbers, insignificant for the instability. Numerical calculations also show that Eqs. (13) and (15) give the same results for the unstable parts of the dispersion diagrams, confirming that the simplified dispersion relation Eq. (15) provides an adequate description of the instability.

On the other hand, the temporal gain depends on the slab thickness, as shown in Fig. 5 for the tanh-mode and coth-mode. We took $f_p=1$ THz, $\varepsilon_d=1$ for Fig. 5(a) and $\varepsilon_d=11.6$ for Fig. 5(b), and the remaining parameters from Table I. When the thickness is large, the gains of both modes are equal, and they remain constant until the thickness decreases to approximately 100 nm. As the thickness decreases further, the gain of the tanh-mode decreases, whereas that of the coth-mode increases. This behavior is due to the reduced plasma frequency, see Eq. (21), which now depends on the slab thickness. For the coth-mode the reduced plasma frequency increases with decrease of the thickness, hence the growth of the gain. For the tanh-mode, the opposite happens.

The dependence of the maximal gain on the thickness is more pronounced for higher permittivity. For 50-nm-thick slabs, the difference between the gains of the coth-mode and tanh-mode for $\varepsilon_d=11.6$ is 0.05 THz, Fig. 5(b), whereas it is only about 0.01 THz for $\varepsilon_d=1$, Fig. 5(a).

When the slab thickness is small, the interaction between the waves propagating on the different surfaces leads to the field distributions in the slab in the form of hyperbolic sine and cosine functions. Outside the slab, the fields decay exponentially. At any value of the wave number, k_z, four waves will propagate. Each wave will generally have its own frequency, given by Eq. (13), and field distribution. We are interested, however, only in the growing wave. Figure 6 shows the field distributions for the tanh-mode and coth-mode of the growing wave for $f_p=1$ THz, $\varepsilon_d=1$, and $d=100$ nm; the wave number chosen is $k_z=0.008\,54\pi/a$ yielding $f\approx(5.62-j0.38)$ THz. The distributions of E_z and E_x are of the same type as those of nondrifting SPPs,[20] but the distributions of H_y, being discontinuous at the boundary,

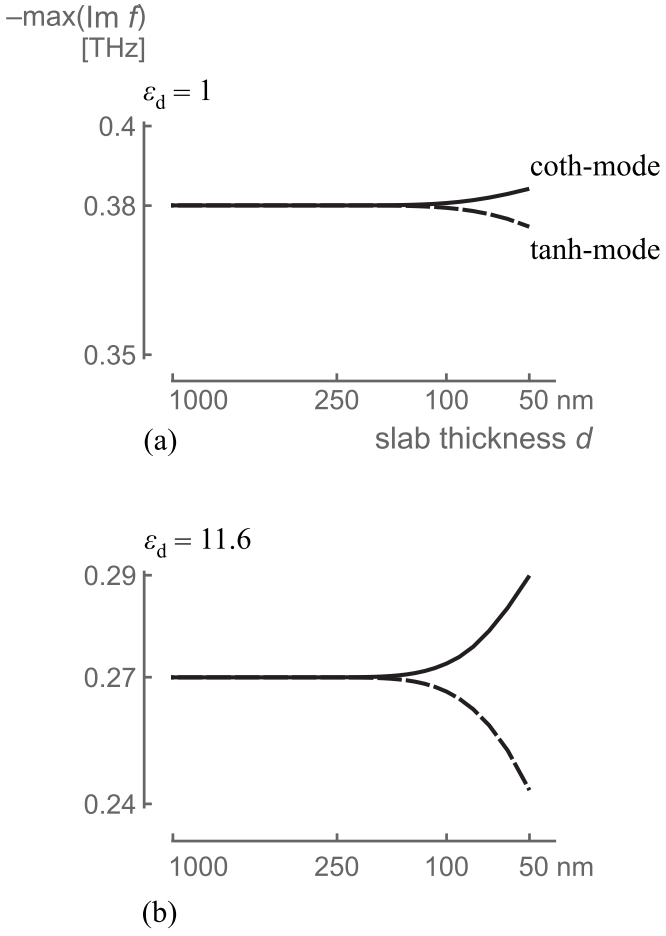

FIG. 5. The maximum of temporal gain as a function of slab thickness: different behavior of the tanh-mode and coth-mode.

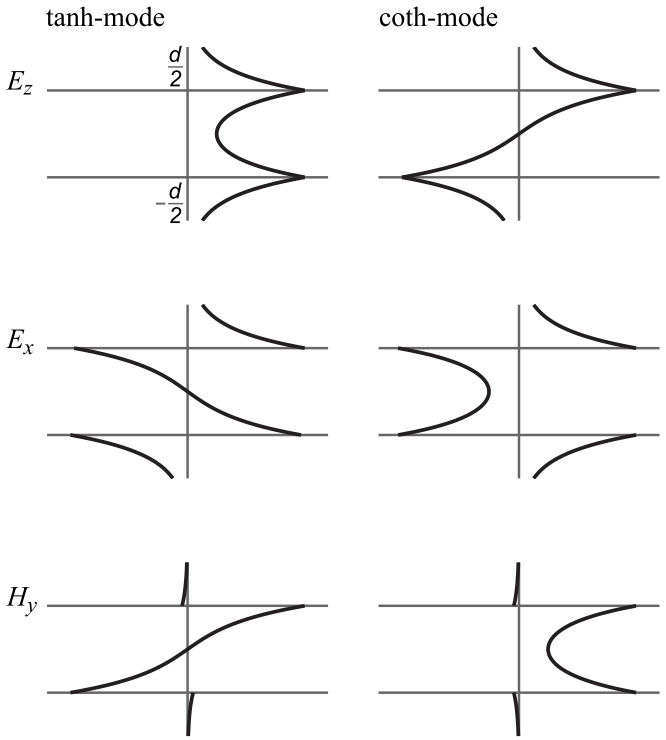

FIG. 6. For the growing wave, the distributions of E_z and E_x fields follow the usual surface-wave patterns. The distribution of the H_y field is discontinuous due to the surface current appearing as a result of the electron drift.

are different. This discontinuity is born by the ac surface current, which changes the boundary conditions in the presence of drift, see Eq. (11).

IV. CONCLUSIONS

In contrast to an unbounded semiconductor, where the instability arises due to the interaction of bulk waves, the instability in the semiconductor slab is due to the interaction of surface waves: surface plasmon polaritons and surface optical-phonon polaritons. When the slab thickness is much larger than the wavelength, the dispersion relation of the slab differs from that of an infinite material in the frequencies of the waves and the coupling coefficient. The two dispersion relations, however, have the same form, and the properties of optical-phonon instability in the slab are analogous to those in unbounded materials, as considered previously.[17,18] The influence of the Lorentz force upon the instability can be disregarded.

When the slab thickness is small, the analogy with the infinite material breaks down. The temporal gain depends on the slab thickness, and it is different for the two surface-wave modes supported by the slab. Because the gain of the coth-mode, with an asymmetric distribution of the longitudinal electric field E_z, grows as the slab thickness decreases, using this mode might be preferable for practical applications.

For stronger instabilities, one has to choose materials with large plasma frequencies and large differences between the longitudinal and transverse optical-phonon frequencies, see Eq. (20). Whereas, the value of the plasma frequency in a material can be varied by doping, the optical phonon frequencies are fixed. The choice of materials is further reduced by the requirement of having drifting electrons and phonons in the same material. This problem could be overcome by designing stacked structures where optical phonons and drifting electrons are provided by different materials. Such configurations could lead to practical designs of terahertz solid-state oscillators and amplifiers.

ACKNOWLEDGMENTS

We thank R. R. A. Syms for helpful discussions. O.S. gratefully acknowledges financial support of the Royal Society and the Royal Academy of Engineering (Newton International Fellowship) and E.S., that of the Deutsche Forschungsgemeinschaft (SAOT and Emmy-Noether Program).

[1] *Terahertz Optoelectronics*, edited by K. Sakai (Springer, Berlin, 2005).
[2] B. Ferguson and X. Zhang, Nat. Mater. **1**, 26 (2002).
[3] B. Williams, Nat. Photonics **1**, 517 (2007).
[4] J. H. Booske, Phys. Plasmas **15**, 055502 (2008).
[5] M. C. Steel and B. Vural, *Wave Interactions in Solid State Plasmas* (McGraw-Hill, New York, 1969).
[6] M. Dyakonov and M. Shur, Phys. Rev. Lett. **71**, 2465 (1993).
[7] T. Otsuji, Y. M. Meziani, T. Nishimura, T. Suemitsu, W. Knap, E. Sano, T. Asano, and V. V. Popov, J. Phys.: Condens. Matter **20**, 384206 (2008).
[8] A. El Fatimy, N. Dyakonova, Y. Meziani, T. Otsuji, W. Knap, S. Vandenbrouk, K. Madjour, D. Theron, C. Gaquiere, M. A. Poisson, S. Delage, P. Prystawko, and C. Skierbiszewski, J. Appl. Phys. **107**, 024504 (2010).
[9] L. Solymar and E. A. Ash, Int. J. Electron. **20**, 127 (1966).
[10] M. Sumi, Appl. Phys. Lett. **9**, 251 (1966).

[11]S. A. Mikhailov, Phys. Rev. B **58**, 1517 (1998).
[12]R. E. Collin, *Foundations for Microwave Engineering* (Wiley-IEEE, Hoboken, NJ, 2001).
[13]V. L. Gurevich, Sov. Phys. Solid State **4**, 1015 (1962).
[14]J. B. Gunn, Phys. Lett. **4**, 194 (1963).
[15]T. O. Woodruff, Phys. Rev. **132**, 679 (1963).
[16]L. Solymar, Proceedings of the Fifth International Congress of Microwave Tubes, Paris, 1964, p. 501.
[17]S. Riyopoulos, Phys. Plasmas **12**, 070704 (2005).
[18]S. Riyopoulos, Phys. Plasmas **16**, 033103 (2009).
[19]*Surface Polaritons: Electromagnetic Waves at Surfaces and Interfaces*, edited by V. M. Agranovich and D. L. Mills (North-Holland, Amsterdam, 1982).
[20]L. Solymar and E. Shamonina, *Waves in Metamaterials* (Oxford University Press, Oxford, 2009).
[21]M. Glicksman and W. A. Hicinbothem, Phys. Rev. **129**, 1572 (1963).
[22]G. M. Branch and T. G. Mihran, IRE Trans. Electron Devices **2**, 3 (1955).
[23]R. J. Briggs, *Electron-Stream Interaction with Plasmas, Research Monograph No. 29* (MIT, Cambridge, MA, 1964).
[24]J. Dai, J. Zhang, W. Zhang, and D. Grischkowsky, J. Opt. Soc. Am. B **21**, 1379 (2004).